J Comput Neurosci () :
DOI 10.1007/s10827-005-5427-0

Phase resetting and coupling of noisy neural oscillators

Bard Ermentrout · David Saunders

Received: 3 May 2005 / Revised: 19 September 2005 / Accepted: 7 October 2005 / Published online: 20 February 2006

Abstract A number of experimental groups have recently computed Phase Response Curves (PRCs) for neurons. There is a great deal of noise in the data. We apply methods from stochastic nonlinear dynamics to coupled noisy phase-resetting maps and obtain the invariant density of phase distributions. By exploiting the special structure of PRCs, we obtain some approximations for the invariant distributions. Comparisons to Monte-Carlo simulations are made. We show how phase-dependence of the noise can move the peak of the invariant density away from the peak expected from the analysis of the deterministic system and thus lead to noise-induced bifurcations.

Keywords: Noise · Neural oscillators · Phase resetting · Pulsatile coupling

Introduction

Synchronous neural oscillations are found in many brain areas (Buszaki and Draguhn, 2004). The mechanisms by which neurons synchronize vary depending on the intrinsic properties of the cells and how they are connected (van Vreeswijk et al., 1994; Chow et al., 1998; Jones et al., 2000). One approach to understanding synchrony in experimental preparations is to measure quantitatively the response of a rhythmically firing neuron to brief inputs (Reyes and Fetz, 1993; Stoop et al., 2000; Oprisan and Canavier, 2000; Netoff et al., 2005; Galan et al., 2005). Typically, current is injected into a neuron to make it fire repetitively. Then, brief stimuli are applied to the cell at different times after it spikes to quantify how the inputs alter the timing. Let T denote the time between spikes in the unperturbed neuron (this is the period of firing). An input at phase s after the last spike (that is, occurring at a time sT since the last spike) causes the interspike interval to change to $T'(s)$. The Phase Resetting Curve (PRC) is defined as $\Delta(s) = 1 - T'(s)/T$. If the PRC is positive (negative), then the input makes the spike occur earlier (later) than it would. Once a PRC is computed, it is possible to create networks of oscillators and explore whether or not they synchronize (Mirollo and Strogatz, 1990; Stoop et al., 2000; Oprisan and Canavier, 2000; Goel and Ermentrout 2002; Netoff et al., 2005). The main difficulty in computing neural PRCs is that in many experimental preparations there is a large amount of noise. Thus, in order to make sense of models using experimental PRCs we have to incorporate the noisiness of the system in our analysis. Several groups have recently computed experimental PRCs (Netoff et al., 2005; Galan et al., 2005) and in some cases measured the variance of their PRCs. One important finding in Netoff et al. (2005) is that the variance of the PRC is also timing-dependent.

This paper is organized as follows. We derive the equations for the distribution of phases in noisy phase resetting curves. We provide an example showing that there is a strong phase-dependence on the variance for PRCs of nonlinear oscillators. We numerically solve the distribution equations (which are linear integral equations) and compare them to Monte-Carlo simulations. We then use two different perturbation approaches the approximate the resulting stationary distributions and use these approximations to study how the phase-dependent variance alters the stationary distributions.

B. Ermentrout supported in part by NIMH and NSF.

Action Editor: Wulfram Gerstner

B. Ermentrout (✉) · D. Saunders
Department of Mathematics, University of Pittsburgh,
Pittsburgh, PA 15260, USA
e-mail: bard@math.pitt.edu

Finally, we compare the results of the integral equations to the experimental data in Netoff et al.

Methods

Derivation of the maps

Mirollo and Strogatz (1990) derive maps for pulse-coupled integrate and fire neurons. Similarly, Goel and Ermentrout (2002) derive maps for pairs of oscillators coupled by their PRCs:

$$\begin{aligned}\frac{d\phi_A}{dt} &= \omega_A + \delta(\phi_B)\Delta_A(\phi_A)\\ \frac{d\phi_B}{dt} &= \omega_B + \delta(\phi_A)\Delta_B(\phi_B),\end{aligned} \tag{1}$$

where $\delta(x)$ is the Dirac delta-function. Let $F_{A,B}(x) = x + \Delta_{A,B}(x)$ be the *phase transition curve*. We assume that $F_{A,B}(x)$ are invertible functions which implies that $\Delta'_{A,B}(x)$ cannot be less than -1. If x_n^A is the phase of cell A at the moment right before cell B fires for the nth time (with x_n^B similarly defined), then

$$\begin{aligned}x_{n+1}^A &= \frac{\omega_A}{\omega_B}\left(1 - F_B\left(x_n^B\right)\right) \equiv G_B\left(x_n^B\right)\\ x_{n+1}^B &= \frac{\omega_B}{\omega_A}\left(1 - F_A\left(x_n^A\right)\right) \equiv G_A\left(x_n^A\right)\end{aligned} \tag{2}$$

If the cells are identical ($\omega_A = \omega_B$ and $F_A(\phi) = F_B(\phi)$), then iterates of Eq. (2) are just iterates of the single map:

$$x \to 1 - F(x) = 1 - x - \Delta(x) \equiv G(x).$$

We will focus mainly on the identical cell case. However, in order to look at pairs of excitatory and inhibitory neurons, it will be necessary to return to the general case.

Derivation of the distributions

Noise can appear in a PRC map in many different forms. Most generally, the map is given by

$$x \to B(x, z)$$

where z is a random variable. The simplest assumption would be that $B(x, z) = G(x) + z$ which would represent additive noise that is independent of the phase, x. This case is considered in Lasota and Mackey (1986). The data of Netoff et al. (2005) and simulations discussed below indicate that this is too simple a model, thus we will assume that

$$B(x, z) = G(x) + R(x)z$$

so that there is some phase (x) dependence of the noise. The map is defined on the unit circle, but since we will consider mainly normally distributed noise, we will work on the whole real line to derive a density function. We extend the definition of $B(x, z)$ to the real line by using the periodicity of B with respect to x, $B(x + 1, z) = B(x, z)$. We will then sum the computed density up modulo 1 to obtain a density function on the circle. We follow standard arguments (see, e.g., Lasota and Mackey (1986)) in order to determine the distribution. Consider the random process

$$X_{n+1} = G(X_n) + z_n R(X_n) \tag{3}$$

where z_n are i.i.d. and taken from a distribution with density $Q(z)$. For us, $G(x) \equiv 1 - F(x) = 1 - x - \Delta(x)$. All variables and functions are defined on $\mathbb{R}$ Let $p_n(x)$ be the probability density function for X_n, and $H(x)$ an arbitrary function on $\mathbb{R}$. Then from $E[H(X_{n+1})] = E[H(G(X_n) + z_n R(X_n))]$ we have:

$$\begin{aligned}&\int_{\mathbb{R}} H(x)p_{n+1}(x)dx\\ &\quad= \int_{\mathbb{R}}\int_{\mathbb{R}} H(G(y) + R(y)z))p_n(y)Q(z)dydz\\ &\quad= \int_{\mathbb{R}}\int_{\mathbb{R}} H(x)Q[(x - G(y))/R(y)]p_n(y)/R(y)\,dydx.\end{aligned}$$

(To get the last integral, we let $x = G(y) + R(y)z$ be a change of variables for z.) Since the function $H(x)$ is arbitrary, we must have

$$\begin{aligned}p_{n+1}(x) &= \int_{\mathbb{R}} Q[(x - G(y))/R(y)]p_n(y)/R(y)dy\\ &\equiv \int_{\mathbb{R}} t(x, y)p_n(y)\,dy.\end{aligned} \tag{4}$$

The function $t(x, y)$ is the rate of transition from state y to state x for the discrete time Markov process (4).

We are not actually interested in $p(x)$ since this is the distribution on the real line. Rather, we want

$$P_n(x) \equiv \sum_{j=-\infty}^{\infty} p_n(x + j)$$

which is the probability for x modulo 1. Using Eq. (4) and the fact that $G(x) = 1 - x - \Delta(x)$ we sum the p_n and also rewrite the integral as a sum:

$$\begin{aligned}P_{n+1}(x) = \sum_{j=-\infty}^{\infty}\sum_{k=-\infty}^{\infty}\int_k^{k+1} &\times Q[(x + j + k + y + \Delta(y))/\\ &R(y)]p_n(y)/R(y)\,dy.\end{aligned}$$

Let $y' = k + y$ and use the fact that $\Delta(x)$, $R(x)$ are 1-periodic to obtain:

$$\begin{aligned} &P_{n+1}(x) \\ &= \sum_{j,k} \int_0^1 Q[(x + y' + j + \Delta(y'))/R(y')] \\ &\quad \times p_n(y' - k)/R(y)\, dy \\ &= \int_0^1 \left(\sum_j \frac{Q[(x + y + j + \Delta(y))/R(y)]}{R(y)} \right) P_n(y)\, dy. \end{aligned}$$

Thus, if we define

$$S(x, y) = \sum_{j=-\infty}^{\infty} \frac{Q[(x + y + j + \Delta(y))/R(y)]}{R(y)} \tag{5}$$

then the invariant density satisfies:

$$P_{n+1}(x) = \int_0^1 S(x, y) P_n(y)\, dy. \tag{6}$$

Note that the function $S(x, y)$ is doubly periodic with period 1.

Numerical calculation of P_n

The function $S(x, y)$ is an infinite sum but since $Q(x)$ vanishes as $|x| \to \infty$, we can truncate the infinite sum and not lose to much accuracy. The integral in Eq. (6) is found by discretizing the density into M bins of size $1/M$ and computing the appropriate sum:

$$\int_0^1 S(x, y) P(y)\, dy \approx \frac{1}{M} \sum_{j=0}^{M-1} S\left(\frac{i}{M}, \frac{j}{M}\right) P^j.$$

Since S does not depend on P we can evaluate $S(x, y)$ at the $M \times M$ grid points and the iteration (6) is reduced to a simple matrix multiplication. Since $S \geq 0$ and has a spectral radius of 1, the iteration (6) will converge to the stationary distribution. We generally use $M = 100$ and obtain convergence to a stationary density in 200–500 iterations. This is completed in less than a second, so that the invariant densities can be computed much faster than the Monte Carlo simulations. Furthermore, we can use the integral equations to develop approximate expressions for the stationary phase distributions.

Simulations

The maps (3) are iterated for 500000 steps and the results are binned into histograms after throwing out the first 100000 iterations. In order to show that there is phase-dependence on the variance of phase-resetting curves, we compute the PRC for a noisy neuron model by stimulating with a brief timed pulse. We use a simple model due to Izhikevich (2003) as our neuron:

$$\frac{dV}{dt} = V^2 + I - u + \sigma dz$$

$$\frac{du}{dt} = a(bV - u)$$

such that when $V = 10$, V is reset to c and u is incremented by d. We used $I = 0.1$, $a = 0.05$, $b = 1$, $c = -1$, and $d = 0.2$. This produces an oscillation with a period of about 22 msec. dz is a white noise process. We solve this using the Euler method with a time step of 0.005 msec. The PRC is computed by perturbing the V equation by a square pulse of duration 0.2 msec and with amplitude 0.5. At each simulation, we start $V(0) = -1$ and $u(0) = 0.43$ which is the value of the variables immediately after resetting. The time for $V(t)$ to reach 10 is computed, T_{10} and the PRC is thus:

$$\text{PRC} = 1 - T_{10}/T$$

where T is the unperturbed period. The mean and the variance of the PRC over 500 trials are computed at each time of the perturbation. The PRC is computed in time steps of 0.2 msec from 0 to 22 msec after the spike.

In all of our example maps, we use a simple model for the PRC and the phase-dependence of the PRC:

$$\Delta(x) = A \sin 2\pi x + B(1 - \cos 2\pi x) + C \sin 4\pi x \tag{7}$$

and

$$R(x) = \sigma[1 + D \sin(2\pi x + \phi)]. \tag{8}$$

Noise is normally distributed with unit variance.

Results

The variance of PRCs is phase-dependent.

Netoff et al. (2005, Figure 5) show that the PRCs which they compute from their hippocampal neurons have a clear dependence of the variance on the phase. In particular, the variance decreases with the time of the spike. Theoretically, the variance and the mean of the PRC should be periodic functions of the time since spiking but it is very difficult to get accurate spike times when the stimulus occurs late in the spiking phase (John White, personal communication). To see if this phenomena can be simply explained and to justify the

assertion that there is phase-dependence, we computed the PRC for a noisy neural model. Figure 1 shows an example of this calculation. The noise is small, but sufficient to cause a rather broad range in the spike times due to any single perturbation (A). The mean has almost exactly the same shape as the mean expected from the deterministic system and does not seem to depend on the noise since it is the same when the noise is doubled (B). Panel C shows the standard deviation for two different noise strengths, $\sigma = 0.02$ and $\sigma = 0.04$. In the former case, we have multiplied the standard deviation by 2 to show that the shape of this curve is independent of the noise up to scaling. There is an obvious dependence of the variability on the time of the spike but the relationship is not entirely clear. Figure 1D shows a plot of the standard deviation against the mean which indicates roughly that there is a 90 degree phase-shift between the two. One would be tempted to suggest that the standard-deviation varies like the derivative of the PRC, but the dependence is more subtle than that. An adequate theory of this dependence remains to be discovered.

Analysis I. Moderate noise

We cannot find closed form solutions to the stationary PDFs in Equation (6). However, if we assume that $R(x)$ is close to 1 and $\Delta(x)$ is small, then we can find a good approximation to $P(x)$ which also provides insight into qualitative changes of $P(x)$ as parameters vary. Recall that the invariant density satisfies:

$$P(x) = \int_0^1 \sum_{j=-\infty}^{\infty} \frac{Q([x+y+j+\Delta(y)]/R(y)}{R(y)} P(y)\, dy$$
$$= \int_{-\infty}^{\infty} \frac{Q([x+y+\Delta(y)]/R(y)}{R(y)} P(y)\, dy$$

where we have "unwrapped' the sum. We keep $P(x)$ as a periodic solution with period 1. We write

$$R(x) = 1 + \epsilon r(x)$$

and assume that $\Delta(x)$ is also $0(\epsilon)$ where $0 < \epsilon \ll 1$. We also assume that $Q(x)$ has variance σ^2. We now expand $P(x)$ is a series in ϵ:

$$P(x) = P_0(x) + \epsilon P_1(x) + \epsilon^2 P_2(x) + \cdots$$

To lowest order:

$$P_0(x) = \int_{-\infty}^{\infty} Q(x+y) P(y)\, dy.$$

The solution to this equation is $P_0(x) = 1$. (This is what you would expect if the PRC was zero and there was no phase-dependence on the noise; the stationary phase is uniform.) The next order equation is:

$$P_1(x) - \int_{-\infty}^{\infty} Q(x+y) P_1(y)$$
$$= \int_{-\infty}^{\infty} Q'(x+y)\Delta(y) dy$$
$$- \int_{-\infty}^{\infty} [Q(x+y) + (x+y)Q'(x+y)] r(y) dy.$$

We change variables in the right-hand integrals $x + y \to y'$ and then, noting that $Q(y) + yQ'(y) = (yQ(y))'$, integrate by parts yielding

$$P_1(x) - \int_{-\infty}^{\infty} Q(x+y) P_1(y) dy$$
$$= -\int_{-\infty}^{\infty} Q(y)\Delta'(y-x) dy + \int_{-\infty}^{\infty} yQ(y) r'(y-x) dy. \quad (9)$$

This is a linear inhomogeneous equation which can be solved by Fourier series. We write

$$\Delta(x) = a_0 + \sum_{n=1}^{\infty} a_n \cos 2\pi nx + b_n \sin 2\pi nx$$

$$r(x) = c_0 + \sum_{n=1}^{\infty} c_n \cos 2\pi nx + d_n \sin 2\pi nx$$

$$P_1(x) = \sum_{n=1}^{\infty} \alpha_n \cos 2\pi nx + \beta_n \sin 2\pi nx$$

and define

$$q_n = \int_{-\infty}^{\infty} Q(x) \cos 2\pi nx\, dx$$
$$s_n = \int_{-\infty}^{\infty} xQ(x) \sin 2\pi nx\, dx.$$

We have assumed that $Q(x)$ is symmetric in order to simplify the analysis, but asymmetric noise could also be analyzed. We note that for normally distributed noise ($Q(x)$ is Gaussian),

$$q_n = \exp(-n^2\pi^2\sigma^2)$$
$$s_n = \pi\sigma^2 n q_n$$

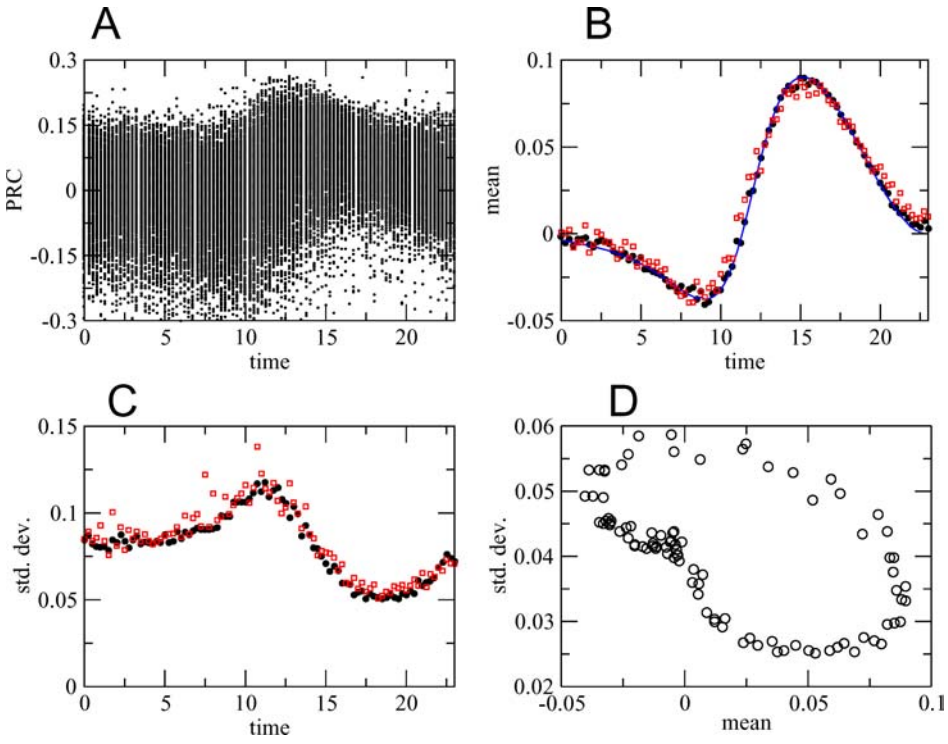

Fig. 1 Phase resetting curves for the Izhikevich model. (A) Data for $\sigma = 0.02$; (B) Mean of the data in (A) (black circles), mean for $\sigma = 0.04$ (red squares), and the noise-free PRC (thin blue line); (C) Standard deviation of the data in (A) (black circles) scaled by a factor of 2 and the standard deviation for a simulation with $\sigma = 0.04$ (red squares); (D) standard deviation against the mean for data in (A)

Plugging in the expansions for $P_1(x)$, $\Delta(x)$, $r(x)$, we find:

$$\alpha_n = -\frac{2\pi n}{1-q_n}[q_n b_n + s_n c_n]$$
$$\beta_n = -\frac{2\pi n}{1+q_n}[q_n a_n - s_n d_n]. \quad (10)$$

We can now use this expression to gain some insight into the form of the stationary state. We consider several different examples.

Example 1

We consider the simplest scenario in which the PRC is a pure sinusoid and there is no phase-dependence of the variance. Thus, we have $\Delta(x) = \epsilon b_1 \sin 2\pi x$ and thus:

$$P(x) = 1 - 2\pi\epsilon b_1 \frac{q_1}{1-q_1} \cos 2\pi x.$$

If $b_1 > 0$ then the deterministic map has a stable fixed point at $x = 1/2$ and we see that the $P(x)$ is also peaked at $x = 1/2$. When $b_1 < 0$, the peaks of $P(x)$ occur at $x = 0,1$ corresponding to a stable synchronized state. Figure 2A shows three curves for $\sigma = 0.2$, $b_1 = 1$, and $\epsilon = 0.02$ corresponding to the approximation, the solution to the integral equation and the Monte-Carlo simulation.

Example 2

Next, we look at the behavior when there are two Fourier modes and the deterministic system has multiple stable phase-locked states. We note that this type of behavior has been seen in several models, notably, the integrate and fire model with excitatory coupling (van Vreeswijk, et al., 1994). Figure 2B shows a simulation with $\epsilon = 0.02$, $\sigma = 0.2$, and $b_2 = 1$, $b_1 = -0.25$. There are two peaks to the invariant density corresponding to asymmetric locked states between the oscillators. This can be destroyed if the noise is increased because the term q_2 goes to zero as σ increases faster than q_1 so that order two harmonic is washed out leaving a stable synchronous state.

Example 3

We now use the approximation to study the effects of phase-dependent variance on the stationary behavior. In particular, we demonstrate a noise-dependent switch from antiphase to synchrony. We suppose that $\Delta(x) = \epsilon b_1 \sin 2\pi x$ as in the first example and $R(x) = 1 + \epsilon c_1 \cos 2\pi x$ with Gaussian noise. From (10) we find

$$P(x) = 1 - 2\pi\epsilon \frac{q_1 b_1 + s_1 c_1}{1-q_1} \cos 2\pi x.$$

This density has a peak at either $x = 0$ (synchrony) or at $x = 1/2$ (antiphase). Since the noise is Gaussian, the peak of

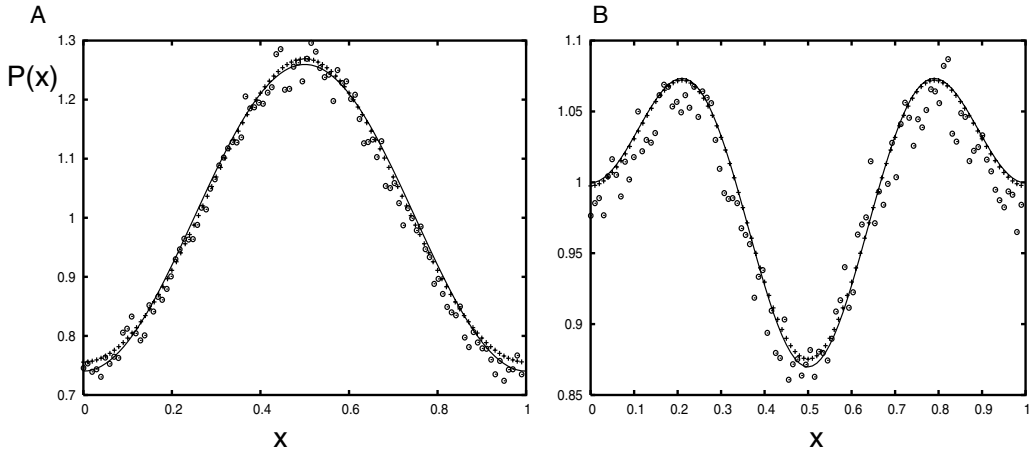

Fig. 2 Comparison of the approximation, the invariant density, and the Monte Carlo simulations for (A) $\sigma = 0.2$, $b_1 = 1$, $\epsilon = 0.02$; (B) $\sigma = 0.2$, $b_1 = -0.25$, $b_2 = 1$, $\epsilon = 0.02$.

the density depends only on the sign of

$$b_1 + \sigma^2 \pi c_1.$$

By choosing b_1 and c_1 to have opposite signs, we can change the amount of noise, σ to effect a switch in stationary phase-loked behavior. The critical value of the noise is

$$\sigma^* = \sqrt{-\frac{b_1}{\pi c_1}}.$$

For example if $c_1 = -0.25$ and $b_1 = 0.05$, then the critical noise level is $\sigma^* \approx 0.252$. Figure 3 shows the result for both the numerical and the analytic calculation. Unlike Example 2, the bifurcation is not one that could be "predicted' from the deterministic dynamics. In the present example, anti-phase is the only stable behavior and changing b_1 only modulates the amplitude (unless of course b_1 changes sign). For $\sigma = 0.25$ which is very close to the bifurcation point, the density is almost flat (Fig. 3B).

Analysis II. Weak noise

If the noise is small, that is, $0 < R(x) \ll 1$ then we expect that the PDF will be sharply peaked around the stable phase-locked states of the deterministic system. A standard approximation is to assume that the PDF consists of a sum of Gaussians centered at the mean phase-locked states with some variance, v:

$$P(x) = C \sum_{i=1}^{k} \frac{e^{(x-m^i)^2/v^i}}{\sqrt{v^i}} \tag{11}$$

where C is a normalization constant, m^i, v^i unknown parameters corresponding to the dynamics of the map. In the appendix, we use the Gaussian approximation to derive the dynamics of the stationary values of m, v:

$$m_{n+1} = G(m_n) + G''(m_n)v_n/2 \tag{12}$$

$$v_{n+1} = R(m_n)^2 + v_n \left(G'(m_n)^2 + R'(m_n)^2 + R(m_n)R''(m_n)\right) \tag{13}$$

This map is quite useful as it can be used to study bifurcations and the shapes of the PDF. Periodic points of this map correspond to peaks in the stationary distribution.

We consider the following model:

$$\Delta(x) = 0.02 \sin 2\pi x + 0.02(1 - \cos 2\pi x) + c \sin 4\pi x$$
$$R(x) = 0.025[1 + 0.5 \sin(2\pi x + 4.55)].$$

The parameters for Δ are chosen so that for c negative or very small and positive, the noiseless system has a stable anti-phase state which undergoes a period doubling bifurcation as c increases (that is, $G'(\bar{m}) = -1$). Parameters for $R(x)$ are chosen so that with a flat PRC the systems settles into a synchronous state. (Here, because the noise is so low, the phase-dependence of the noise makes little difference.)

For small noise, away from the bifurcation point, we can estimate the variance for the map as:

$$\bar{v}_{\text{app}} = \frac{R(\bar{m})^2}{1 - G'(\bar{m})^2}. \tag{14}$$

For $c = -.04$, the approximation yields $\bar{v}_{\text{app}} = 0.00166$ and the true value is $\bar{v} = 0.00164$. When $c = 0.008$ (very close to the bifurcation point for the deterministic system), the

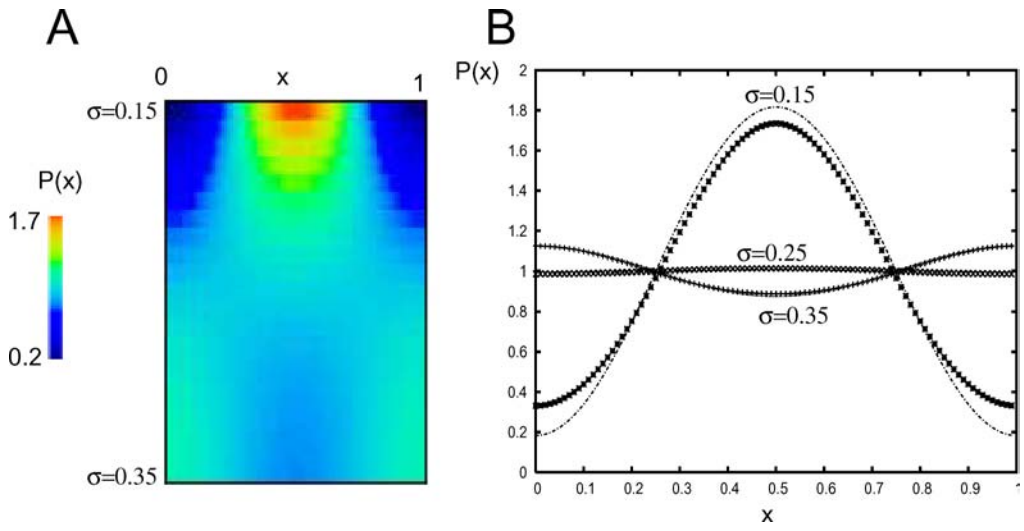

Fig. 3. Noise-induced bifurcation from anti-phase to synchrony. (A) Plot of the stationary density as a function of the noise (increasing along the vertical axis). (B) Three examples from (A) comparing the numerical density with the approximation.

approximation yields $\bar{v}_{\text{app}} = 0.060$ while the true value is $\bar{v} = 0.039$, a 33% error.

Figure 4(A) shows the Gaussian approximation and the numerical solution of the PDF when $c = 0.0$ for which the approximate map predicts a single peak. Figures 4(B,C) show the bifurcation diagrams for period two solutions to Eqs. (12)–(13) as the parameter c varies. Near the deterministic bifurcation value $c = 0.02$, there is an abrupt change in the period one solution and the variance increases by two orders of magnitude (panel C). Away from the bifurcation ($c = 0.04$) the variance is again small so that both our simple linear approximation (14) and the Gaussian ansatz work very well as is seen in figure 4D. Here, the map has a period two solution leading to the double peaks in the PDF. We remark that in A, the peak is considerably wider than the peaks in D; this is seen in the variance curve 4C. For c between about 0.007 and $c = .025$, the dynamics are too close to the bifurcation point and the Gaussian approximation breaks down. We also remark that this type of breakdown of the approximation near a bifurcation is not seen in the analysis in the previous section. On the other hand, our prior analysis is only good when the PRC is quite small, while here, no such constraints were necessary.

The Gaussian approximation works even for "exotic" cases. For example, if we take

$$\Delta(x) = 0.04 \sin 2\pi x + 0.16(1 - \cos 2\pi x) + 0.06 \sin 4\pi x$$

and $R(x) = 0.01$ (very small noise), the map (12, 13) has a period 4 fixed point. The Monte-Carlo simulation (400000 steps) show 4 peaks in the stationary distribution. Both the position of the peaks and their width is matched as can be seen in Figure 5.

Application to experimental data

We can apply the thory to experimental data. Figure 6 shows the results of this. In A,B we show polynomial fits for the PRC and the standard deviation as a function of the phase for excitatory and inhibitory stimuli. In the experiments, cells in the hippocampus were driven to fire at a regular rate and stereotyical EPSPs and IPSPs were applied at different times after a spike. For EPSPs, the PRC is typical of that seen in theoretical models. However for IPSPs the PRC does not vanish at 1. This is likely due to the difficulty in resolving the precise spike time when the stimulus occurs near the natural (unperturbed) period (John White, private communication). Figure 6B shows that there is only a small phase-dependence for IPSP input standard-deviation while the phase-dependence for EPSPs can be rather substantial. Figure 6(C, D)show the predicted phase relationships for a pair of mutually coupled cells in absence of noise. EPSPs tend to synchronize while IPSPs result in an alternating rhythm. Figures 6Ei,ii show the invariant density using the functions in A, B. In addition we show that for EPSP stimuli, the phase-dependence of the noise has a small effect on the invariant density (compare dashed and solid line in 6Ei). While these effects are not as dramatic as those in the toy models, the results show that phase-dependent noise can shift the timing between pairs of coupled oscillators.

Netoff et al. (2005) also look at heterogeneous pairs in which once cell sends EPSPs to the other while receiving IPSPs. So far, our methods have been applied to identical cells. There is no reason why heterogenous networks cannot also be analyzed. Consider Eq. (2). Recall that x^A is the phase of cell A when cell B has fired and vice-versa. Equation (2) has a noisy analogue. Instead of the deterministic phase-transition curve, $F_A(x_A)$), we have the noisy one $F_A(x^A) +$

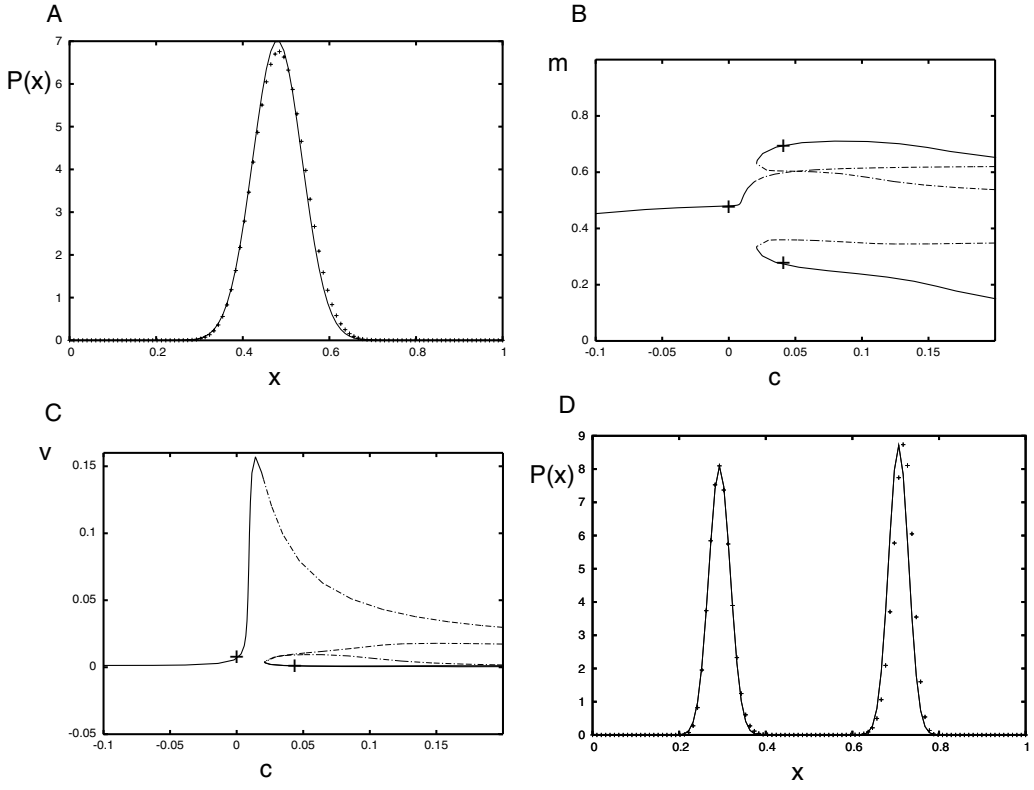

Fig. 4 Low noise approximation and the numerically computed PDF. Here $\Delta(x) = 0.02 \sin 2\pi x + 0.02(1 - \cos 2\pi x) + c \sin 4\pi x$, $R(x) = \sigma(1 + 0.5 \sin(2\pi x + 4.55))$, $\sigma = 0.025$ (A) Numerically computed PDF and the Gaussian approximation computed form equations (12) and (13) for $c = 0$. (B) Bifurcation diagram for the map (12, 13) as c is varied. The left branch of solutions corresponds to a single peak PDF and right two branches correspond to a double peak At $c \approx 0.02$ the double peak solution undergoes a saddle-node and the single-peak solution undergoes a Hopf (Neimark-Sacker) bifurcation. Crosses indicate $c = 0.0$ and $c = 0.04$. (C) Variance as the parameter c is varied. Crosses show $c = 0.0$ and $c = 0.04$ corresponding to (A) and (D) respectively. (D) The numerical solution of the PDF for $c = 0.04$ and the Gaussian approximation using the mean and variance from the map

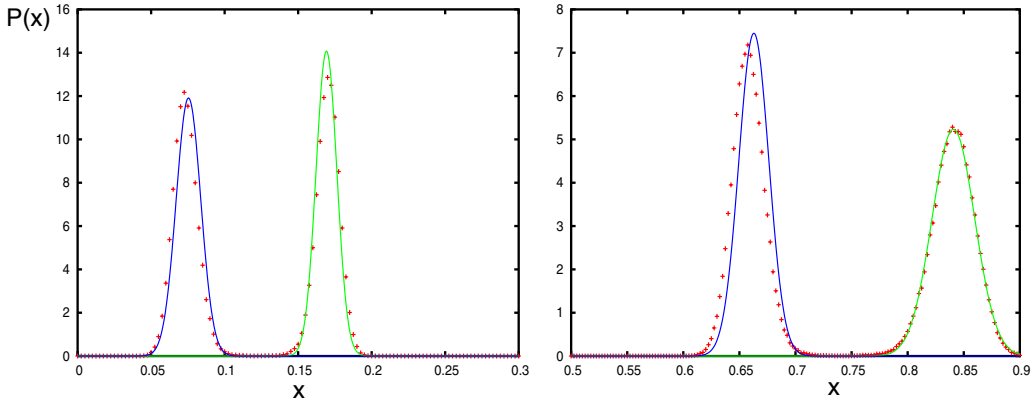

Fig. 5 Example of a period four solution to the simple PRC model with very low noise. + symbols are the result of a Monte Carlo simulation broken into 400 bins. Solid lines are the Gaussian approximation with the mean and variance obtained from iterations of Eqs. (12, 13) Note that in order to improve the comparison, we have broken up the full distribution into two pieces and have used a different vertical scale

$\xi^A R_A(x^A))$ where ξ^A is a random variable with zero mean. Thus, the noisy heterogenous dynamics are given by:

$$x^A_{n+1} = \frac{\omega_A}{\omega_B}\left(1 - F_B\left(x^B_n\right) - \xi^B_n R_B\left(x^B_n\right)\right)$$

$$x^B_{n+1} = \frac{\omega_B}{\omega_A}\left(1 - F_A\left(x^A_n\right) - \xi^A_n R_A\left(x^A_n\right)\right).$$

If we assume that $\xi^{A,B}$ come from identical symmetric distributions, then we can readily derive equations for $P^{A,B}(x)$,

the density of the phases. This results in a pair of coupled integral equations for the probabilities of $x^{A\,B}$:

$$P^A_{n+1}(x) = \int_0^1 S^B(x,\,y)P^B_n(y)dy \tag{15}$$
$$P^B_{n+1}(x) = \int_0^1 S^A(x,\,y)P^A_n(y)dy$$

where

$$S^B(x,\,y) = \frac{\omega_B}{\omega_A} Q\left[\left(\frac{\omega_B}{\omega_A}x - 1 + F_B(y)\right)\Big/ R_B(y)\right]\Big/ R_B(y)$$
$$S^A(x,\,y) = \frac{\omega_A}{\omega_B} Q\left[\left(\frac{\omega_A}{\omega_B}x - 1 + F_A(y)\right)\Big/ R_A(y)\right]\Big/ R_A(y).$$

Figure 6E(iii,iv) depicts the stationary distributions for an excitatory-inhibitory pair. That is, cell A is excitatory and cell B is inhibitory. $P_e(x)$ is the density of the phase of the excitatory cell at the moment the inhibitory cell fires and $P_i(x)$ is the phase density for the inhibitory cell at the moment the excitory cell fires. We note that the E cell lags the I cell slightly because the IPSPs can only delay the onset of a spike (Figure 6A). Similarly, the I cell leads the E cell since EPSPs advance the spike time (except for a narrow window near the beginning of a cycle, cf. Figure 6A). The two distributions are not simple reflections of each other since the effects of the coupling are not symmetric.

Discussion

We have developed a method to compute various probabilistic quantities which arise in the study of coupled neural oscillators. Previous work on the questions of oscillator synchrony in the presence of noise has mainly been applied to differential equations models (Sompolinsky et al., 1991; Tass 2003; Acebron et al., 2005; Strogatz, 2000,). For neurons coupled in a pulsatile manner, maps are a more natural setting. The methods here can be used in conjunction with experimental studies. It is now possible to create artificially coupled networks with real cells using a method called the dynamic clamp (Netoff et al., 2005). Thus, the techniques derived in this paper can be applied to experimental synchronization of noisy neurons. There are several adavantages of the integral equations over Monte-Carlo simulations. First, it is not easy to determine how many iterations to run; this can depend on both the amplitude of the noise and the intrinsic dynamics. The integral equations are exact and can be solved very quickly by iteration. More importantly, the deterministic nature of the integral equations allowed us to develop a simple perturbation scheme to approximate the invariant density.

Throughout the paper, we have made a number of assumptions about both the PRCs and the form of the noise in order to derive simple models for the phase densities. The assumptions on the PRCs are necessary in order to have well-defined maps even in absence of the noise. For a single forced oscillator, the invertibility requirement for the phase-transition curve (PTC : F(x) = x + Δ(x)) can be relaxed (Stoop et al., 2000). But for coupled oscillators, stronger coupling forces one to make additional assumptions about the behavior of the oscillators. A classic example is the work of Mirollo and Strogatz (1990) which considered strong phase-resetting. They make the assumption of absorption—if an oscillator is induced to fire immediately, then it is absorbed into the group of synchronous oscillators. This assumption is not robust to noise or to heterogeneity. In the experiments of Netoff et al. (2005), and Galan et al. (2005) the stimuli are sufficiently weak so that the PTC is invertible. However, the PRCs computed by Reyes and Fetz (1993) have a slope of -1 near the time of firing which means that they fire as soon as stimulated. Thus, the function $F(x)$ is not invertible for their experiments. We have also assumed that the PRCs are memoryless: the effect of a stimulus lasts for only one cycle. For weak stimuli, this is a reasonable assumption, but for stronger stimuli, such as in Reyes and Fetz (1993), the phase continues to evolve over at least two cycles. We chose a simple additive noise model simply because this is the same model that Netoff et al. (2005) used to fit their dynamic clamp. We need not make this assumption in order to derive the densities. If we consider a more general form of the map, say $x \to B(x, z)$ where z is a random variable, then we can still derive an equation for the invariant density provided we can solve $B(x, z) = y$ for z. It remains to be seen if the simple additive assumption holds in other experiments.

One of our most interesting findings is that phase-dependent noise can change the peaks of the PDF so that they can be substantially moved from the deterministic locked state. In one example, the noise induced a switch from synchrony to anti-phase. It is not clear how strong this effect will be in experimental models although there is a shift in the peak of the phase distribution in the Netoff data (see Figure 6Ei). Any nonlinear oscillator driven with a small amount of noise appears to have phase-dependence of the variance of the PRC, so that the existence of this dependence should come as no surprise. However, in most theoretical studies of noisy phase-locking this dependence is ignored. An adequate theory which explains the relationship between the variance and the mean remains to be found although progress on some simple cases has been made (Doiron and Ermentrout, in preparation).

We have not applied the analytic methods to heterogeneous networks although the techniques are obviously extendable. For example, if the noise is weakly dependent on the phase, the frequencies of the two oscillators are close,

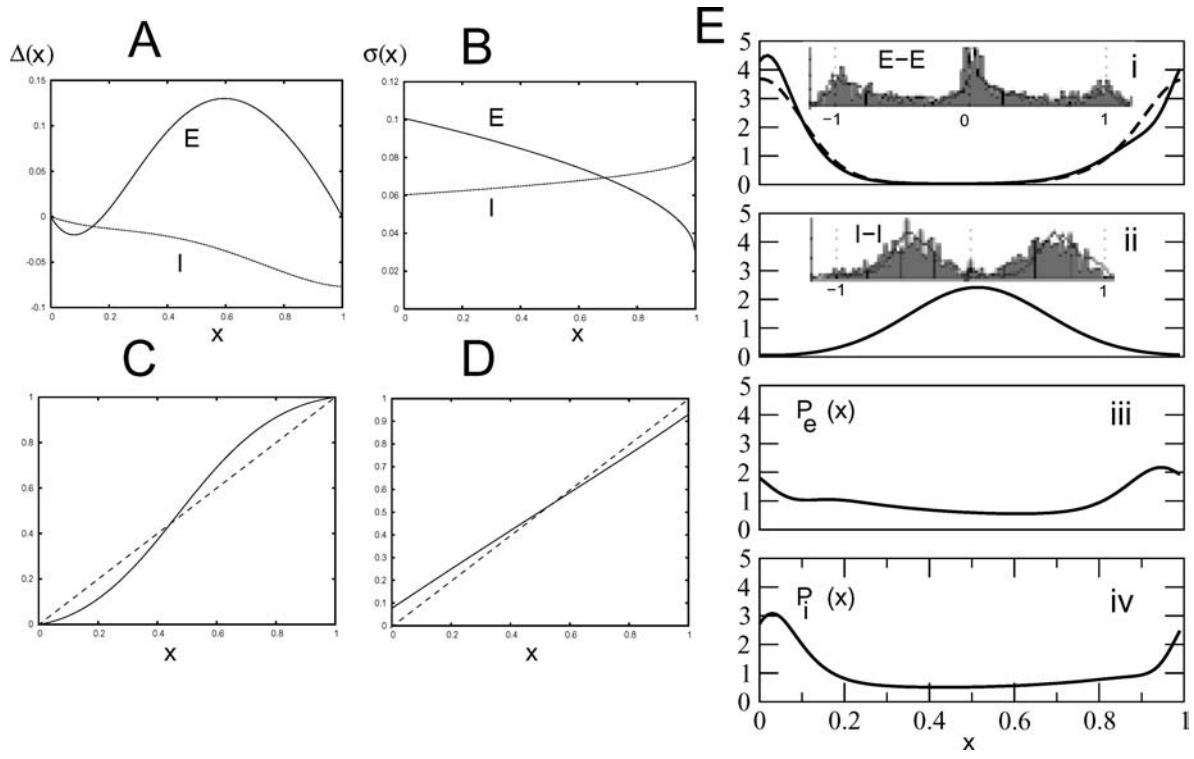

Fig. 6 Application of the theory to the results of Netoff et al. (2005). (A) Polynomial fit to the experimental PRCs (provided by Theoden Netoff) E-excitatory stimulus, I = inhibitory. (B) The standard deviation as a function of the phase for the excitaory and inhibitory stimuli. (C) Fixed points for mutual excitatory coupling in absence of noise. (D) Fixed points for mutual inhibitory coupling in absence of noise. (E) Invariant densities from (6) for excitatory and inhibitory coupling (i,ii) and for mixed coupling (iii,iv, see text). In (i) the dashed line depicts the invariant density for a constant (rather than phase-dependent) variance

and the PRCs are small, then the lowest order solutions to (15) will be $P^j(x) = 1$. The next order terms can be solved using Fourier series just as the homogeneous case was.

Another case which should be amenable to analysis is the "all-all" model in the limit as there are infinitely many oscillators. Ariaratnam and Strogatz (2001) recently gave a complete analysis of the all-all model:

$$\frac{dx_i}{dt} = \omega_i - \frac{K}{N}\sum_{j=1}^{N} a_m(1+\cos x_j)^m \sin x_i$$

for $m = 1$ (with numerical support in the case $m > 1$). If $m \to \infty$, the coupling becomes a delta function. Thus, it is likely that their methods could be applied to our situation. The analysis of any other networks (small N or local coupling) is probably best handled with a Monte Carlo simulation.

How does this approach compare or differ from weakly coupled noisy oscillators? Suppose that the PRC is small (as we assumed for the perturbation methods) and the oscillators are identical. Then Eq. (1) can be averaged leading to

$$\frac{d\phi_A}{dt} = \omega + \Delta(\phi_A - \phi_B) + dW_A$$

$$\frac{d\phi_B}{dt} = \omega + \Delta(\phi_B - \phi_A) + dW_B$$

where we have added an independent source of noise to each oscillator. Letting $\psi = \phi_B - \phi_A$ denote the phase-difference between the oscillators, it is easy to derive a Fokker-Planck equation for the distribution of the phase differences (Gardiner, 1997) and from this extract the stationary PDF:

$$P(\psi) = A\exp(-H(\psi)/\sigma^2)$$

where

$$H(\psi) = \int_0^{\psi} \Delta(x) - \Delta(-x)dx$$

and A is a normalization constant. The peaks and valleys of $P(\psi)$ correspond to zeros of the odd part of the PRC. There is clearly no phase-dependence of the noise amplitude in this model. Thus, for example, in the case of I-I coupling in Netoff et al. (2005), this simple model is probably a good predictor of the stationary PDF, but would fail in the example illustrated in Figurei 3. Similarly, for the weak noise case, this expression fails to capture the complexity of, say, Fig.

5 which arises due to the *finite* (as opposed to infinitesimal) nature of the coupling. Thus, while there have been numerous papers on weakly coupled noisy phase-locking, there are aspects of the problem which are best captured by maps and the integral equations which arise from these maps.

Appendix

Here we fill in the details of the analytic calculations for weak noise in the main text. We start with the noisy map with normally distributed noise:

$$x_{n+1} = G(x_n) + R(x_n)\xi_n$$

and assume that the PDF is a gaussian with mean m_n and variance v_n. Rodriguez and Tuckwell (1996) make a similar assumption in their analysis of the role of noise in the Fitzhugh-Nagumo equations. This approach applied to differential equations is reviewed in Lindner et al. (2004). Here we follow their methods applied to maps. The mean satisfies the equation:

$$m_{n+1} = E[G(x_n)]$$

which is exact since the expected value of the noisy part is zero. The variance satisfies

$$\begin{aligned} v_{n+1} &= E\left[x_{n+1}^2\right] - E[x_{n+1}]^2 \\ &= E[\{G(x_n) + R(x_n)\xi_n\}^2] - m_n^2 \\ &= E[G(x_n)^2] + E[R(x_n)^2] - E[G(x_n)]^2. \end{aligned}$$

As with the mean, this expression is also exact. The challenge is to approximate the expectations. To do this, we write:

$$\begin{aligned} G(x) = \;& G(m + x - m) \approx G(m) + G'(m)(x - m) \\ & + G''(m)(x - m)^2/2 + \cdots \end{aligned}$$

We use the fact that $v = E[(x - m)^2]$ so that the mean satisfies:

$$m_{n+1} = G(m_n) + G''(m_n)v/2. \tag{16}$$

This is an approximate expression since we have truncated to linear order in the variance. Applying the same methods to the variance, we find

$$v_{n+1} = R(m_n)^2 + v_n(G'(m_n)^2 + R'(m_n)^2 + R(m_n)R''(m_n)). \tag{17}$$

Note that one could continue the series to get higher order accuracy, but for our purposes, this is sufficient.

Acknowledgments We'd like to thank Theoden Netoff and John White for graciously providing the formulas for the fits to their experimental data. BE thanks Mike Mackey for references to the integral equations and Brent Doiron for related conversations.

References

Acebron JA, Bonilla LL, Prez Vicente, CJ, Ritort F, Spigler R (2005) The Kuramoto model: A simple paradigm for synchronization phenomena. Reviews of Modern Physics 77: 137–185.

Ariaratnam JT, Strogatz SH (2001) Phase diagram for the Winfree model of coupled nonlinear oscillators. Phys. Rev. Lett. 86: 4278–4281.

Buzsaki G, Draguhn A (2004) Neuronal oscillations in cortical networks. Science 304: 1926–1929.

Chow CC, White JA, Ritt, J, Kopell N (1998) Frequency control in synchronized networks of inhibitory neurons. J. Comput. Neurosci. 5: 407–420.

Ermentrout B, Pascal M, Gutkin B (2001) The effects of spike frequency adaptation and negative feedback on the synchronization of neural oscillators. Neural Computation 13: 1285–1310.

Galan RF, Ermentrout GB, Urban NN (2005) Efficient estimation of phase-resetting curves in real neurons and its significance for neural-network modeling. Phys. Rev. Lett. 94: 158101.

Gardiner CW (1997) Handbook of Stochastic Methods (2nd edition). Springer, New York.

Goel P, Ermentrout B (2002) Synchrony, stability, and firing patterns in pulse-coupled oscillators Physica D 163: 191–216.

Izhikevich EM (2003) Simple model of spiking neurons. IEEE Transactions on Neural Networks 14: 1569–1572.

Jones SR, Pinto DJ, Kaper TJ, Kopell N (2000) Alpha-frequency rhythms desynchronize over long cortical distances: A modeling study. J. Comput. Neurosci. 9: 271–91.

Lasota A, Mackey MC (1986) Chaos, Fractals and Noise: Stochastic Aspects of Dynamics, Springer Applied Mathematical Science 97. Springer-Verlag, Berlin (Chapt. 10.5).

Lindner B, Garcia-Ojalvo J, Neiman A, Schimansky-Geier L (2004) Effects of noise in excitable systems, Phys. Rep. 392, 321.

Mirollo RM, Strogatz SH (1990) Synchronization of pulse-coupled biological oscillators. SIAM. J. Appl. Math. 50: 1645–1662.

Netoff TI, Banks MI, Dorval AD, Acker CD, Haas JS, Kopell N, White JA (2005) Synchronization in hybrid neuronal networks of the hippocampal formation. J. Neurophysiol. 93: 1197–208.

Oprisan SA, Canavier CC (2000) Phase response curve via multiple time scale analysis of limit cycle behavior of type I and type II excitability. Biophys. J. 78: 218–230.

Reyes AD, Fetz EE (1993) Effects of transient depolarizing potentials on the firing rate of cat neocortical neurons. J. Neurophysiol. 69: 1673–183.

Rodriguez R, Tuckwell HC (1996) Statistical properties of stochastic nonlinear dynamical models of single spiking neurons and neural networks. Physical Review E 54: 5585–5590.

Sompolinsky H, Golomb D, Kleinfeld D (1991) Phase coherence and computation in a neural network of coupled oscillators. In: Non-Linear Dynamics and Neural Networks, H.G. Schuster and W Singer Eds. (VCH, Weinheim, 1991), pp. 113–140.

Stoop R, Schindler K, Bunimovich LA (2000) Neocortical networks of pyramidal neurons: From local locking and chaos to macroscopic chaos and synchronization. Nonlinearity 13: 1515–1529.

Strogatz, S (2000) From Kuramoto to Crawford: Explaining the onset of synchronization in populations of globally coupled oscillators. Physica D 143: 1–20.

Tass PA (2003) Stochastic phase resetting of two coupled phase oscillators stimulated at different times. Phys. Rev. E 67:05 1902.

Van Vreeswijk C, Abbott LF, Ermentrout GB (1994) When inhibition not excitation synchronizes neural firing. J. Comput. Neurosci. 1: 313–321.